NEUROSCIENCE

Astrocytes contribute to pain gating in the spinal cord

Qian Xu[1,2], Neil C. Ford[3], Shaoqiu He[3], Qian Huang[3], Michael Anderson[1], Zhiyong Chen[3], Fei Yang[3], LaTasha K. Crawford[4], Michael J. Caterina[1,4,5], Yun Guan[3,5]*, Xinzhong Dong[1,2,5]*

Various pain therapies have been developed on the basis of the gate control theory of pain, which postulates that nonpainful sensory inputs mediated by large-diameter afferent fibers (Aβ-fibers) can attenuate noxious signals relayed to the brain. To date, this theory has focused only on neuronal mechanisms. Here, we identified an unprecedented function of astrocytes in the gating of nociceptive signals transmitted by neurokinin 1 receptor–positive (NK1R$^+$) projection neurons in the spinal cord. Electrical stimulation of peripheral Aβ-fibers in naïve mice activated spinal astrocytes, which in turn induced long-term depression (LTD) in NK1R$^+$ neurons and antinociception through activation of endogenous adenosinergic mechanisms. Suppression of astrocyte activation by pharmacologic, chemogenetic, and optogenetic manipulations blocked the induction of LTD in NK1R$^+$ neurons and pain inhibition by Aβ-fiber stimulation. Collectively, our study introduces astrocytes as an important component of pain gating by activation of Aβ-fibers, which thus exert nonneuronal control of pain.

INTRODUCTION

The gate control theory of pain proposed by Melzack and Wall (*1*) in 1965 provided a mechanism to explain pain inhibition by peripheral nonnoxious input. Various pain therapies that use neurostimulation of Aβ-fibers have been developed since the establishment of this theory, such as spinal cord stimulation and peripheral nerve stimulation (*2*, *3*). To date, our understanding of how these therapies alleviate pain has been based solely on neuronal mechanisms as postulated by this theory.

Peripheral sensory neurons, whose cell bodies reside in the dorsal root ganglion (DRG) and trigeminal ganglion, detect and transmit sensory information from the periphery to the central nervous system (CNS). These neurons and their afferent nerves consist of diverse types. Most large myelinated afferents (Aβ-fibers) are low-threshold mechanoreceptors that mediate nonpainful signals. Most of the thinly myelinated afferents (Aδ-fibers) and unmyelinated afferents (C-fibers) are thermoreceptors or nociceptors, which detect and transmit painful signals (*4*, *5*). Most Aδ- and C-fibers terminate in the superficial spinal cord (laminae I and II), whereas Aβ-fibers project into deeper laminae III to V. In the spinal cord, painful signals are modulated by local interneurons before being sent to the brain via projection neurons (*6*, *7*). Approximately 80% of lamina I projection neurons are neurokinin 1 receptor–positive (NK1R$^+$) neurons (*8*, *9*) and play a pivotal role in the transmission of noxious stimuli (*10*, *11*).

The gate control theory proposed that input from nonpainful Aβ-fibers closes the "gate" by activating spinal inhibitory interneurons, thereby attenuating pain signals transmitted by projection neurons to the brain (*12*, *13*). Although neuronal mechanisms of spinal pain gating have been comprehensively studied (*14*–*17*), the role of glial cells has been largely overlooked. Astrocytes, which are widely located in the CNS, provide various types of metabolic support to neurons and contribute to information processing within neuronal circuits by modulating neuronal excitability and synaptic transmission (*18*, *19*). Mounting evidence suggests that astrocytes can be activated by multiple neurotransmitters and, in turn, secrete glial transmitters such as adenosine 5′-triphosphate (ATP), glutamate, D-serine, and γ-aminobutyric acid (GABA) (*20*–*23*). Thus, astrocytes play a critical role in pain modulation (*24*–*26*).

Most studies have suggested that activation of astrocytes facilitates or enhances pain transmission (*24*, *25*). Here, we show that astrocyte activation by Aβ-fiber stimulation can directly inhibit spinal NK1R$^+$ projection neurons. Electrical stimulation (50 Hz) of Aβ-fibers in naïve mice activated astrocytes from deep laminae to the superficial spinal cord. These activated astrocytes acted as a gate by inducing long-term depression (LTD) in NK1R$^+$ projection neurons and inhibited pain through endogenous adenosinergic mechanisms. Thus, our new model introduces spinal astrocytes as an important component of pain gating, increasing our understanding of the nonneuronal gate control mechanisms.

RESULTS

Aβ-stimulation activates astrocytes in the deeper laminae followed by those in superficial laminae of dorsal horn

Previous studies used glial fibrillary acidic protein (GFAP)–GCaMP6 mice, in which GCaMP6s is expressed in astrocytes under GFAP-Cre control to study astrocyte function in the spinal cord (*27*, *28*). To visualize astrocyte activity, we used two-photon in vivo calcium imaging of the spinal cord in GFAP-GCaMP6s mice (Fig. 1A). Double staining of spinal cord slices showed that GFAP-Cre labeled most GFAP immunoreactivity–positive astrocytes [0.72 correlation coefficient (CC)] but few Iba1-positive microglia (0.28 CC) and NeuN-positive neurons (0.22 CC; fig. S1). When 50-Hz low-intensity (20 μA) electrical stimulation was applied to the sciatic nerve to activate Aβ-fibers (*29*), fluorescence intensity increased in the superficial dorsal horn (laminae I to II) of GFAP-GCaMP6 mice, indicating an activation of astrocytes (Fig. 1, B and C). In this in vivo preparation, only fluorescence signals from superficial dorsal horn can be monitored. Because Aβ-fibers project mainly into the deeper dorsal horn (e.g., laminae III to V), we postulated that Aβ-stimulation may

[1]The Solomon H. Snyder Department of Neuroscience, Center for Sensory Biology, Johns Hopkins University School of Medicine, Baltimore, MD, USA. [2]Howard Hughes Medical Institute, Johns Hopkins University School of Medicine, Baltimore, MD, USA. [3]Department of Anesthesiology and Critical Care Medicine, Johns Hopkins University School of Medicine, Baltimore, MD, USA. [4]Department of Biological Chemistry, Johns Hopkins University School of Medicine, Baltimore, MD, USA [5]Department of Neurological Surgery, Johns Hopkins University School of Medicine, Baltimore, MD, USA.
*Corresponding author. Email: xdong2@jhmi.edu (X.D.); yguan1@jhmi.edu (Y.G.)

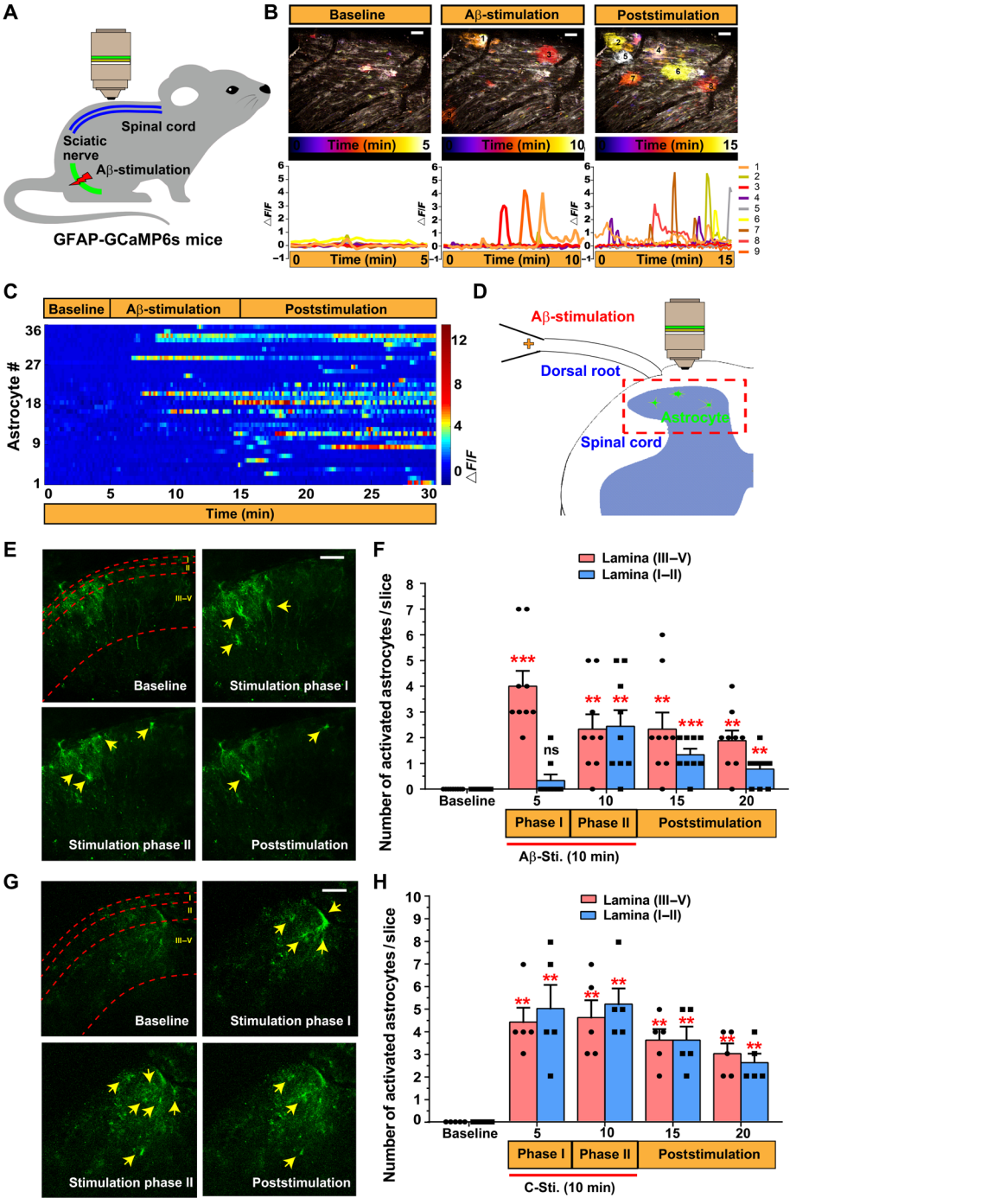

Fig. 1. Aβ-stimulation activates spinal astrocytes in deep laminae followed by those in superficial laminae. (**A**) Schematic of two-photon microscopy setup for imaging spinal astrocytes in live GFAP-GCaMP6s mice. After stable baseline recording, the sciatic nerve was stimulated with 50-Hz electrical stimulation at Aβ-fiber intensity (20 μA, 0.1 ms, and 10 min) during live imaging. (**B**) Time-lapse color-coded images (top) and GCaMP6 traces (bottom) before (left), during (middle), and after (right) 50-Hz Aβ-stimulation of the sciatic nerve in anesthetized mice. Nine activated astrocyte clusters in the visual field were identified during and after Aβ-stimulation. Scale bars, 50 μm. (**C**) Heatmap representation of calcium responses from 36 astrocytes in superficial laminae. $N = 4$ mice. (**D**) Schematic diagram illustrates confocal imaging setup for spinal cord slice preparations from GFAP-GCaMP6s mice. Aβ-stimulation (50 Hz, 10 μA, 0.1 ms, and 10 min) was administered to the ipsilateral dorsal root through a suction electrode. (**E**) Representative fluorescence images show acute activation of deep lamina astrocytes followed by activation of superficial astrocytes. Stimulation time is divided into phase I (0 to 5 min) and phase II (5 to 10 min). Arrows indicate activated astrocytes. Scale bar, 50 μm. (**F**) Population data showing the number of activated astrocytes ($n = 9$ slices from six mice). (**G**) Representative fluorescence images show acute, simultaneous activation of deep lamina astrocytes and superficial astrocytes by C-fiber intensity stimulation of dorsal root. Stimulation time is divided into phase I (0 to 5 min) and phase II (5 to 10 min). Arrows indicate activated astrocytes. Scale bar, 50 μm. (**H**) Population data showing the number of activated astrocytes in deep and superficial laminae ($n = 5$ slices from three mice). Data are presented as means ± SEM, paired *t* test; $^{**}P < 0.01$ and $^{***}P < 0.001$; ns, not significant.

activate astrocytes in the deeper laminae first. To test this possibility, we performed GCaMP imaging of transverse spinal cord slices with dorsal root attached. Applying Aβ-stimulation at the dorsal root activated astrocytes in the deeper laminae before those in superficial laminae I to II (Fig. 1, E and F). However, applying high-intensity electrical stimulation, which excites both A- and C-fibers in the dorsal root, activated astrocytes in deep and superficial laminae nearly simultaneously (Fig. 1, G and H). Aβ-strength stimulation activated an average of 6.56 astrocytes in each spinal cord slice (n = 9 slices), and C-strength stimulation activated an average of 12.00 astrocytes (n = 5 slices). In addition, by stimulating the spinal cord slices with bath-applied BzATP [agonist of P_2X_7 purinergic receptor expressed only in glial cells; (*30*)], we determined that astrocytes activated by Aβ-stimulation represent 11.29% of the total astrocyte population (fig. S2, A and B).

Aβ-stimulation induces LTD of excitatory synaptic transmission in NK1R$^+$ neurons

During spinal nociceptive transmission, NK1R$^+$ neurons in the superficial laminae act as vital relays for ascending pain signals to reach the brain (*6*, *9*). Therefore, we generated NK1R-CreGFP transgenic mice (Cre and GFP fusion protein expression under NK1 promotor control) to examine the functional relationship between spinal astrocytes and NK1R$^+$ neurons during nociceptive transmission. The histochemical results indicated that NK1R$^+$ neurons were distributed in lamina I, lamina III, and deeper laminae (Fig. 2A). Colocalization experiments suggested that 64.86% of CreGFP in NK1R-CreGFP knock-in mice are NK1R immunoreactivity–positive neurons (fig. S3, A and B). In addition, the injection of Cholera Toxin Subunit B dye at parabrachial nuclei retrogradely labeled 57.69% of NK1-CreGFP$^+$ neurons in the spinal cord, indicating that they are projection neurons (fig. S4, A and B). By patch-clamp recording of excitatory postsynaptic currents (EPSCs), we showed that in response to test stimulation, NK1R$^+$ neurons in lamina I received C-fiber inputs with 100% monosynaptic transmission and Aβ-fiber inputs with 76% polysynaptic transmission (fig. S5, A and B). These data suggest that NK1R$^+$ neurons and incoming C-fibers form direct synapses and that most of the connections between NK1R$^+$ neurons and Aβ-fibers are indirect. In our study, we recorded NK1R-GFP neurons, which represent a small subset of lamina I neurons.

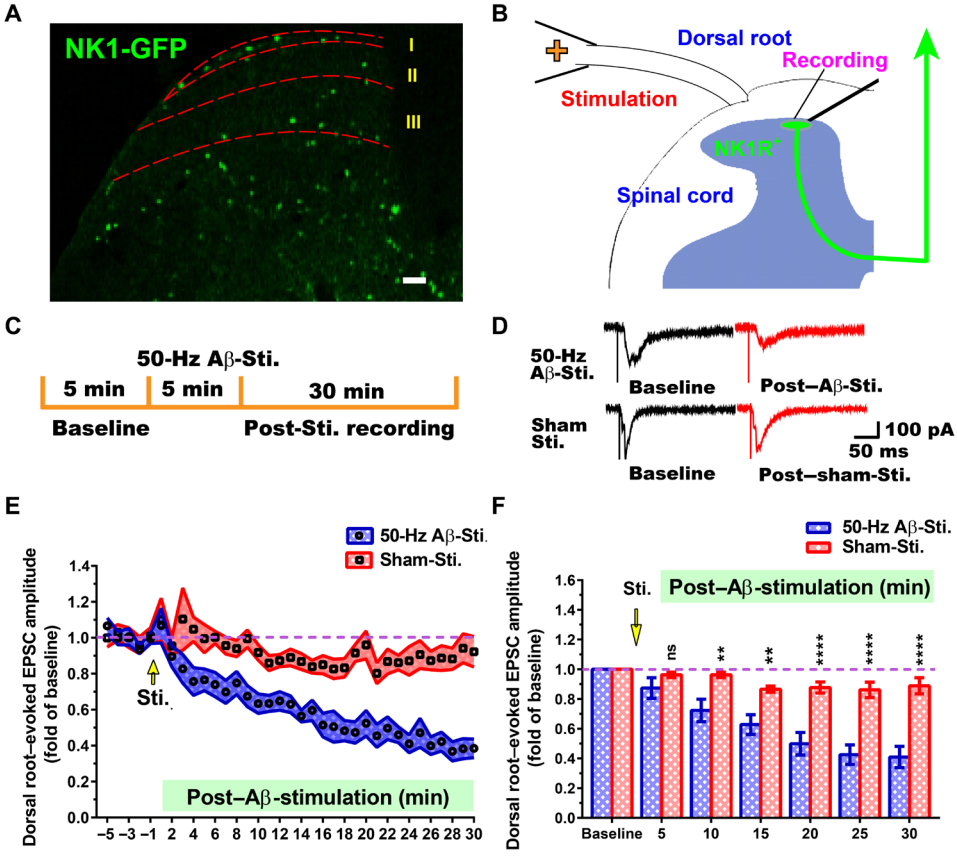

Fig. 2. Aβ-stimulation induces LTD of C-fiber–evoked EPSCs (C-eEPSCs) in NK1R$^+$ neurons. (**A**) GFP-Cre is knocked in to the NK1 gene. NK1-GFP neurons are present mainly in lamina I, lamina III, and deeper laminae of the spinal cord. Scale bar, 100 μm. (**B**) Schematic diagram illustrates patch clamp recording from a spinal cord slice. Electrical Aβ-stimulation (Sti., 50 Hz, 10 μA, 0.1 ms, and 5 min) or a high-threshold test pulse (500 μA, 0.1 ms) was applied to the ipsilateral dorsal root through a suction electrode. (**C**) Protocol of electrical Aβ-stimulation that induced LTD in NK1R$^+$ neurons in spinal cord slices. First, eEPSC baseline was recorded for 5 min. Then, Aβ-electrical stimulation was delivered to the ipsilateral dorsal root. Last, poststimulation C-eEPSCs were recorded for 30 min after Aβ-stimulation. (**D**) Representative traces show eEPSCs in lamina I NK1$^+$ neurons in response to a test pulse before (black) and after (red) Aβ- and sham stimulation. (**E**) Time course of C-eEPSC amplitudes before and after Aβ-stimulation (n = 11 slices) and sham stimulation (n = 10 slices). (**F**) The amplitudes of C-fiber eEPSCs during each 5-min period were averaged for analysis. Data are presented as means ± SEM. SEM are shown as shaded range in (E). $^{**}P < 0.01$ and $^{****}P < 0.0001$ by two-way mixed model analysis of variance (ANOVA) followed by Bonferroni post hoc comparisons; ns, not significant.

They are likely a more homogeneous population and/or different from superficial dorsal horn neurons recorded in previous studies. In previous studies (*31*, *32*), lamina I neurons, which may consist of different cell types, were randomly selected for recording, possibly contributing to the differences between our findings and those of prior studies in the percentage of neurons responding to Aβ-stimulation. Aβ-stimulation (50 Hz) induced a slowly developing LTD (lasting >30 min) of evoked EPSCs to C-fiber inputs (C-eEPSCs) in lamina I NK1R$^+$ neurons (Fig. 2, D and E). Furthermore, the paired-pulse ratio increased significantly at 10 min and returned to prestimulation level at 20 min after Aβ-stimulation (fig. S6, A and B). These findings suggest that the prolonged inhibition of C-eEPSCs in NK1R$^+$ neurons by Aβ-stimulation may initially involve a presynaptic mechanism, again highlighting the role of Aβ-fiber inputs in gate control of spinal nociceptive transmission. We selected 50 Hz for Aβ-stimulation because it is the most common frequency used for clinical pain therapy (e.g., dorsal column stimulation). It has been validated in preclinical studies (*29*, *33*–*35*). We also tested 4- and 100-Hz frequencies to examine whether LTD induction by Aβ-stimulation is frequency dependent. In naïve mice, the peak amplitudes of C-fiber eEPSC were progressively decreased by both 50- and 100-Hz Aβ-stimulation, but 4 Hz was ineffective (fig. S7, A to C).

Activation of astrocytes contributes to LTD in NK1R$^+$ neurons after Aβ-stimulation

Two-photon in vivo calcium imaging revealed that pretreatment of the spinal cord with A438079, a blocker of the glial-expressed P2X7 receptor (*36*, *37*), inhibited Aβ-stimulation–induced astrocyte activation (fig. S8, A to C). LTD of C-eEPSCs after Aβ-stimulation was also blocked by A438079 pretreatment (Fig. 3, A and C), suggesting that glial cell activation plays a role in the inhibition of NK1R$^+$ neurons by Aβ-stimulation.

Because P2X7 receptors are expressed in different types of glial cells, we further delineated the involvement of astrocyte activation in LTD of C-eEPSCs induced by Aβ-stimulation. First, we showed that pretreatment of spinal cord slices with the astrocyte-specific toxin L-α-aminoadipate (LAA) inhibited Aβ-stimulation–induced LTD in NK1R$^+$ neurons (*38*, *39*) (Fig. 3, B and C). Second, we injected the dorsal spinal cord with AAV5-GFAP-hM4D(Gi)-mCherry virus to specifically express inhibitory designer receptors exclusively activated by designer drugs (DREADD) human M4 muscarinic (hM4) Di in spinal astrocytes (fig. S9, A and B). Bath application of clozapine *N*-oxide (CNO), which induces astrocytic Gi activation (*40*, *41*), attenuated 50-Hz Aβ-stimulation–induced LTD (Fig. 3, E and F). Last, we used an optogenetic method in which green light shone on spinal cord slices of GFAP-Cre;;Ai39 mice would silence astrocytes. Aβ-stimulation induced LTD of evoked local field potential to C-fiber inputs in superficial dorsal horn of spinal slices, but the effect was blocked by optogenetic silencing of astrocytes (fig. S10, B to D). Collectively, these results from multiple approaches help to unravel the contribution of spinal astrocyte activation to Aβ-stimulation–induced pain gating.

To test whether astrocyte activation also contributes to Aβ-stimulation–induced inhibition of deep dorsal horn neurons, we conducted in vivo recording of wide-dynamic range (WDR) neurons from deep laminae in rats. WDR neurons play an important role in spinal nociceptive transmission, and their responses to a suprathreshold electrical stimulus at the peripheral nerve or receptive field consist of an early A-component and a later C-component (*33*, *42*). Stimulation of Aβ-fibers at 50 Hz on the sciatic nerves inhibited C-component firing. This effect was attenuated by spinal application of LAA, which inhibits astrocyte function (fig. S11). Thus, spinal astrocyte activation by Aβ-stimulation may exert a similar inhibitory effect on nociceptive-processing neurons in deeper laminae, further supporting our main hypothesis.

An endogenous adenosinergic mechanism contributes to Aβ-stimulation–induced LTD of NK1R$^+$ neurons

We next sought to understand the neurochemical mechanisms that underlie Aβ-stimulation–induced astrocyte activation and NK1R$^+$ neuron inhibition. In vivo microdialysis revealed an increased level of ATP in cerebrospinal fluid collected from the lumbar spinal cord after Aβ-stimulation of sciatic nerve in mice (Fig. 4C). ATP may bind to P2X7 receptors to activate glial cells, which in turn release glial transmitters, including ATP (*43*).

ATP can be quickly converted enzymatically to adenosine in the extracellular space (*44*). The level of adenosine was also elevated in the cerebrospinal fluid after Aβ-stimulation (Fig. 4D). A previous study showed that peripheral large fiber activation suppresses spinal dorsal horn neurons through an adenosine mechanism (*45*). However, it is unclear whether adenosine plays a role in astrocyte-mediated neuronal inhibition. We tested this possibility next. Bath application of ARL67156, an ATP-converting enzyme inhibitor (*46*), attenuated LTD in NK1R$^+$ neurons in spinal cord slices after Aβ-stimulation (Fig. 4, H and J). These findings suggest that endogenous adenosine may contribute to LTD induction and that one source may be the ATP that is released during Aβ-stimulation. Immunohistochemistry staining showed that 85.81% of NK1R$^+$ neurons expressed adenosine A1 receptors (Fig. 4E). Application of adenosine to the bath inhibited C-eEPSCs in NK1R$^+$ neurons (Fig. 4, F and G). The A1 receptor antagonist DPCPX (*47*) blocked Aβ-stimulation–induced LTD in NK1R$^+$ neurons (Fig. 4, I and J). Collectively, these findings suggest that Aβ-stimulation may activate spinal astrocytes (likely a subset of astrocytes; see Discussion) and induce release of ATP. ATP is subsequently converted into adenosine, which activates the A1 receptor on NK1R$^+$ neurons, decreasing their excitability.

Our findings suggest that a GABAergic mechanism may also contribute to this form of LTD. Specifically, the $GABA_A$ receptor antagonist bicuculline, but not the $GABA_B$ receptor antagonist CGP 52432, attenuated Aβ-stimulation–induced LTD in NK1R$^+$ neurons (fig. S12, A to C). Furthermore, in addition to the aforementioned astrocytic mechanism, we cannot rule out the possible involvement of microglial cells in Aβ-stimulation–induced inhibition of NK1R$^+$ neurons, as minocycline, which inhibits microglial activation, also blocked Aβ-stimulation–induced inhibition (fig. S13, A and B).

Glial activation contributes to Aβ-stimulation–induced pain inhibition

To directly test the role of spinal astrocyte activation in pain inhibition produced by electrical Aβ-stimulation, we conducted pain behavior tests in mice. Mice that were lightly anesthetized with 1% isoflurane received Aβ-stimulation (50 Hz, 0.2 ms, and 20 μA) through a pair of hook electrodes at the sciatic nerve for 10 min. They recovered from anesthesia within 10 min after completing Aβ-stimulation and wound closure. Paw withdrawal latency to radiant heat stimulation was measured at 30, 60, and 120 min after Aβ-stimulation. Compared to sham stimulation, electrical

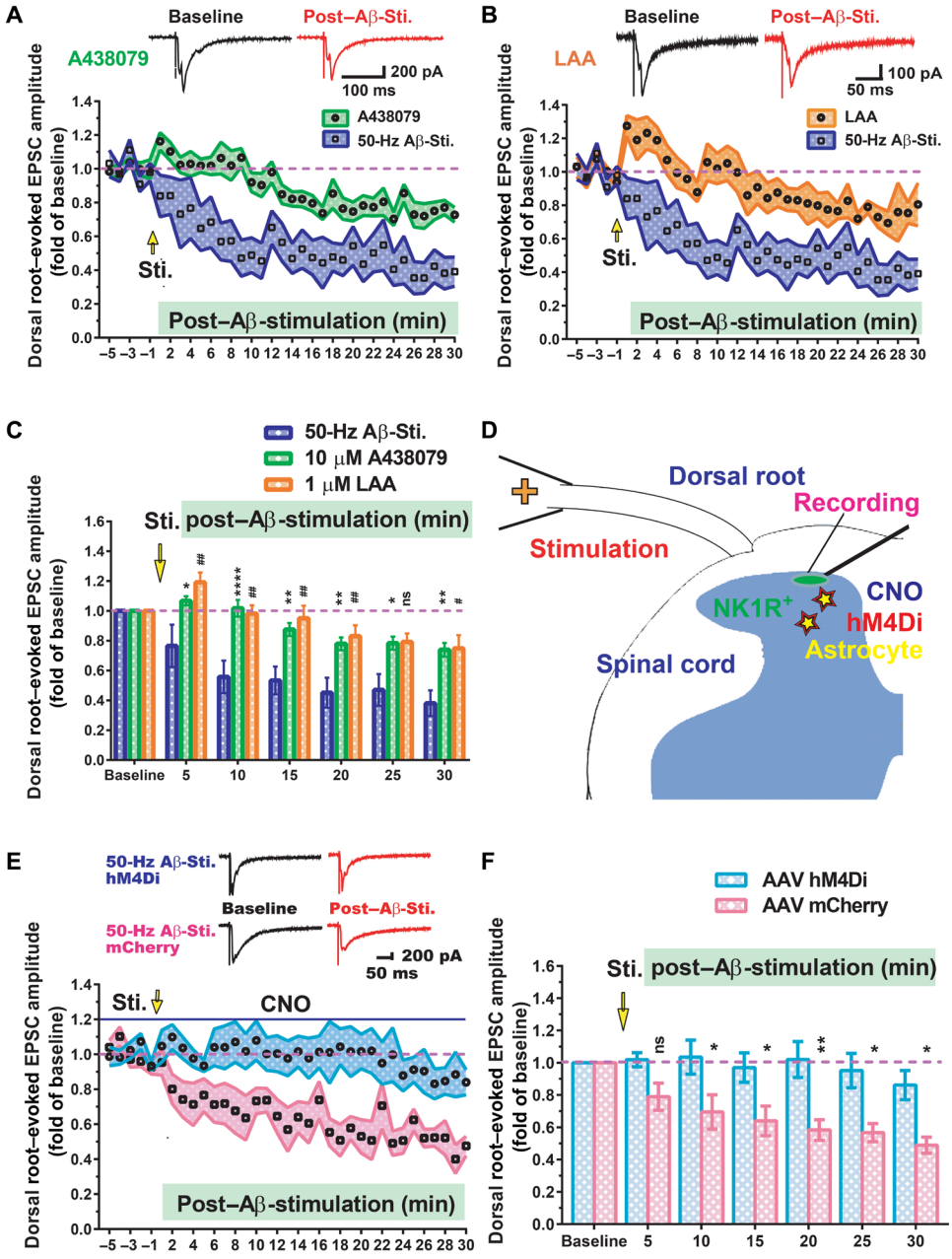

Fig. 3. Astrocytes are the gate for LTD in NK1R$^+$ neurons after Aβ-stimulation. (**A** and **B**) C-eEPSC amplitudes were measured before and after Aβ-stimulation ($n = 9$ slices) in spinal cord slices that had been exposed to P2X7 antagonist A438079 (10 μM, A) or astrocyte-specific inhibitor LAA (1 mM; B) for 30 min by bath application. Insets: individual eEPSC traces recorded before (black) and after (red) Aβ-stimulation. (**C**) Quantification of data in (A) and (B). A438079 partially blocked the Aβ-stimulation–induced LTD. The significant inhibition appeared within the first 5 min and lasted for 30 min. Similar to A438079, LAA partially blocked the Aβ-stimulation–induced LTD. The significant inhibition appeared within the first 5 min and lasted for 30 min. (**D**) Schematic diagram illustrates patch clamp recording from a spinal cord slice. hM4D(Gi) was expressed on spinal astrocytes through intraspinal injection of AAV5-GFAP-hM4D(Gi)-mCherry virus into NK1-GFP-Cre mice 3 weeks before patch clamp recording. (**E**) Time course of C-eEPSC amplitudes before and after Aβ-stimulation in AAV5-GFAP-hM4D(Gi)-mCherry virus–injected ($n = 10$ slices) and control AAV5-GFAP-mCherry virus–injected ($n = 7$ slices) groups that received bath application of CNO (1 μM). Insets: individual eEPSC traces before and after Aβ-stimulation in hM4Di (top) and control (bottom) groups. (**F**) Quantification of data in (D). Astrocytic Gi activation with CNO blocked the Aβ-stimulation–induced LTD. Data are presented as means ± SEM. SEM are shown as shaded range in (A), (B), and (E). *$P < 0.05$, **$P < 0.01$, ****$P < 0.0001$, #$P < 0.05$, and ##$P < 0.01$ versus the respective control by two-way mixed model ANOVA followed by Bonferroni post hoc comparisons.

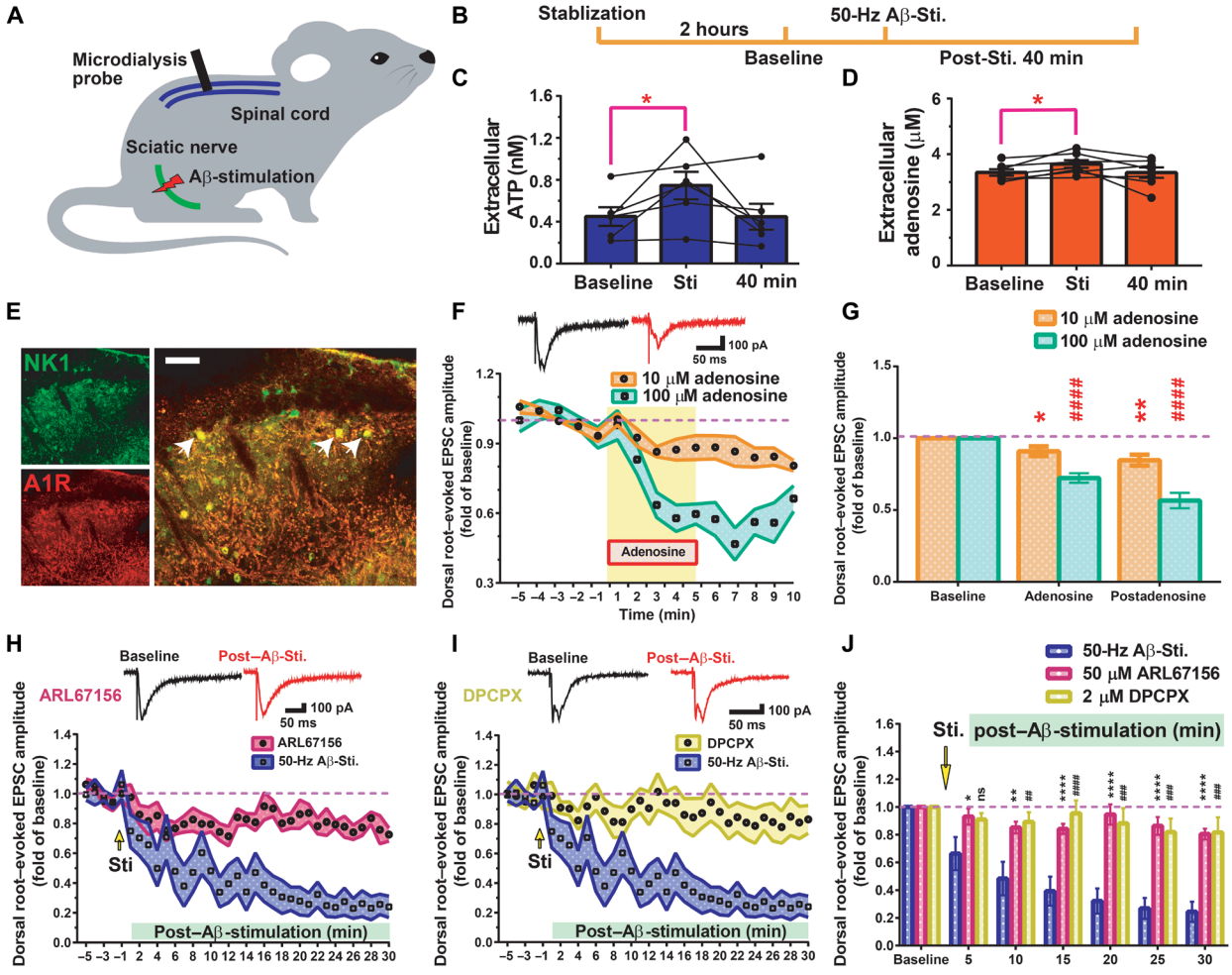

Fig. 4. Adenosinergic mechanism contributes to Aβ-stimulation–induced LTD in NK1R$^+$ neurons. (**A**) Schematic diagram illustrates in vivo microdialysis setup for measuring substance in spinal extracellular fluid. (**B**) Experimental timeline of microdialysis study. The microdialysis probe was inserted into the dorsal horn 2 hours before starting the microdialysis. (**C** and **D**) Quantification of ATP (C) and adenosine (D) in extracellular fluid of spinal cord. $N = 6$ to 7 mice. Both ATP and adenosine levels increased from baseline during 10 min of Aβ-stimulation. Two-way mixed model ANOVA with Bonferroni correction (repeated measure). *$P < 0.05$. (**E**) Representative image shows anti–adenosine A1 receptor antibody staining (arrows) of NK1R$^+$ neurons. Scale bar, 50 μm. (**F**) Time course of C-eEPSC amplitudes in NK1R$^+$ neurons before, during, and after 5-min bath application of 10 μM ($n = 8$ slices) and 100 μM ($n = 9$ slices) adenosine. Inset: Individual eEPSC traces recorded before and after 100 μM adenosine perfusion. (**G**) Adenosine significantly reduced C-eEPSC amplitudes in superficial NK1R$^+$ neurons. *$P < 0.05$, **$P < 0.01$, and ####$P < 0.0001$ versus the respective baseline by paired t test. (**H**) C-eEPSC amplitudes were measured before and after Aβ-stimulation ($n = 7$ slices) to spinal cords that received bath application of adenosine ectonucleotidase antagonist ARL67156 (50 μM). Insets: Individual eEPSC traces. (**I**) C-eEPSC amplitudes were measured before and after Aβ-stimulation ($n = 10$ slices) to spinal cords that received bath application of A1 receptor antagonist DPCPX (2 μM). Insets: Individual eEPSC traces. (**J**) The effect of ARL67156 and DPCPX on C-eEPSC amplitudes of superficial NK1R$^+$ neurons. ARL67156 and DPCPX partially blocked the Aβ-stimulation–induced LTD. Data are presented as means ± SEM. SEM are shown as shaded range in (F), (H), and (I). *$P < 0.05$, **$P < 0.01$, ****$P < 0.0001$, ##$P < 0.01$, ###$P < 0.001$, and ####$P < 0.0001$ versus the respective control by two-way mixed model ANOVA followed by Bonferroni post hoc comparisons.

Aβ-stimulation produced significant heat antinociception that was evident from 30 min through 60 min after application (Fig. 5B).

Using pharmacologic and chemogenetic approaches, we then suppressed astrocyte activation during electrical Aβ-stimulation and the pain test. Pretreating the mice with an intrathecal injection of the astrocyte toxin LAA (100 nmol) significantly reduced Aβ-stimulation–induced heat antinociception, as compared to that with saline pretreatment (Fig. 5C). For chemogenetic inhibition of astrocytes, AAV5-GFAP-hM4D(Gi)-mCherry virus was injected into dorsal lumbar spinal cord 3 weeks before behavior testing to express the inhibitory DREADD on astrocytes. Direct inhibition of astrocytes with CNO also inhibited Aβ-stimulation–induced heat antinociception (Fig. 5D). Thus, pain inhibition from Aβ-stimulation may be dependent, in part, on the activation of spinal astrocytes. Furthermore, pretreatment with an intrathecal injection of the adenosine receptor antagonist DPCPX (10 μg/10 μl) also reduced heat antinociception from Aβ-stimulation (Fig. 5C), again suggesting an adenosinergic mechanism.

To rule out the potential influence of inhalation anesthesia and motor fiber activation during electrical Aβ-stimulation on subsequent animal pain behavior, we used optogenetics to selectively activate sensory Aβ-fibers. We generated MafA-Cre transgenic mice and used AAV1-Ef1a-DIO-ChETA-EYFP virus to selectively express ChETA in a MafA subpopulation of DRG neurons (Fig. 6, A and B).

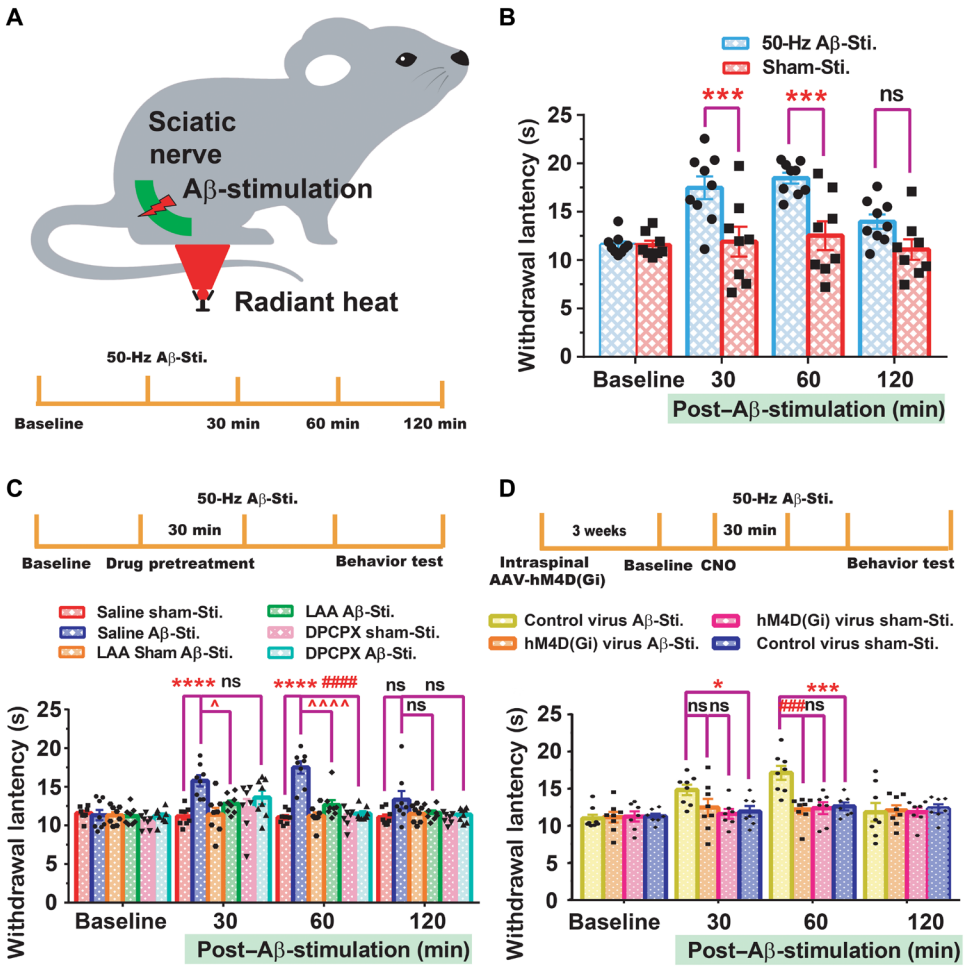

Fig. 5. Activation of astrocytes by Aβ-stimulation inhibits heat nociception. (**A**) Paw withdrawal latency to radiant heat stimulation was measured in wild-type mice at 30, 60, and 120 min after Aβ-electrical stimulation of the sciatic nerve. (**B**) Compared with sham stimulation ($N = 8$ mice), Aβ-stimulation ($N = 9$ mice) produced a significant analgesic effect at 30 and 60 min. (**C**) Saline, LAA, or DPCPX was injected into mice intrathecally 30 min before Aβ-stimulation. Compared with the saline control ($N = 8$ mice), LAA pretreatment ($N = 7$ mice) blocked Aβ-stimulation–induced pain inhibition at 30 min. DPCPX pretreatment blocked pain inhibition at 60 min ($N = 8$ mice). (**D**) AAV5-GFAP-hM4D(Gi)-mCherry virus was injected into the spinal cord 3 weeks before behavior testing. CNO was injected intraperitoneally into GFAP-hM4D(Gi) virus–pretreated mice 30 min before Aβ-stimulation. Silencing of astrocytes in GFAP-hM4D(Gi) mice ($N = 8$ mice) blocked pain inhibition by Aβ-stimulation at 60 min, as compared with that in the control group ($N = 8$ mice). Data are presented as means ± SEM. *$P < 0.05$, ***$P < 0.001$, ****$P < 0.0001$, ###$P < 0.001$, ####$P < 0.0001$, ^$P < 0.05$, and ^^^^$P < 0.0001$ versus respective control groups by two-way mixed model ANOVA followed by Bonferroni post hoc comparisons.

MafA is a transcription factor that is expressed specifically in large-diameter, low-threshold mechanoreceptors (*48*); ChETA is an enhanced version of channel rhodopsin that can follow high-frequency light stimulation (*49*). Consistently, our data showed that 95% of MafA-Cre;Tdtomato–positive neurons in the DRG expressed NF200 (a marker for large-diameter neurons) and that few of these neurons colabeled with markers of nociceptive neurons [calcitonin gene-related peptide (CGRP), 2%; IB4, 5%; fig. S14, A and B]. The peripheral terminals of MafA-positive neurons expressing ChETA could be selectively activated by applying blue light to the hind paw. Ten minutes of photostimulation with 50-Hz blue light inhibited heat nociception in awake naïve mice (Fig. 6C). Consistent with findings from electrical Aβ-stimulation, the pain inhibitory effect from photostimulation was blocked by pretreatment with LAA and DPCPX (Fig. 6D) and reduced by CNO in mice that expressed hM4Di in astrocytes (Fig. 6E). Together, these behavior findings suggest that pain inhibition by both electrical and photostimulation of Aβ-fibers in the sciatic nerve depends on spinal astrocyte activation and involves a spinal adenosinergic mechanism.

In addition to heat pain inhibition, we also determined the contribution of astrocytes to Aβ-stimulation–induced inhibition on mechanical pain. Paw withdrawal frequency to 0.4 and 1 g von Frey monofilament stimulation was significantly decreased between 30 and 120 min after electrical Aβ-stimulation, as compared to that after sham stimulation (fig. S15, A and B). Pretreatment with astrocyte toxin LAA (100 nmol) attenuated this effect, suggesting that mechanical pain inhibition from Aβ-stimulation may also depend on activation of spinal astrocytes (fig. S15, C and D).

DISCUSSION

The findings presented here suggest that electrical Aβ-stimulation at peripheral nerves may activate a subset of astrocytes in the dorsal horn of naïve mice. Aβ-fibers may release multiple neurotransmitters

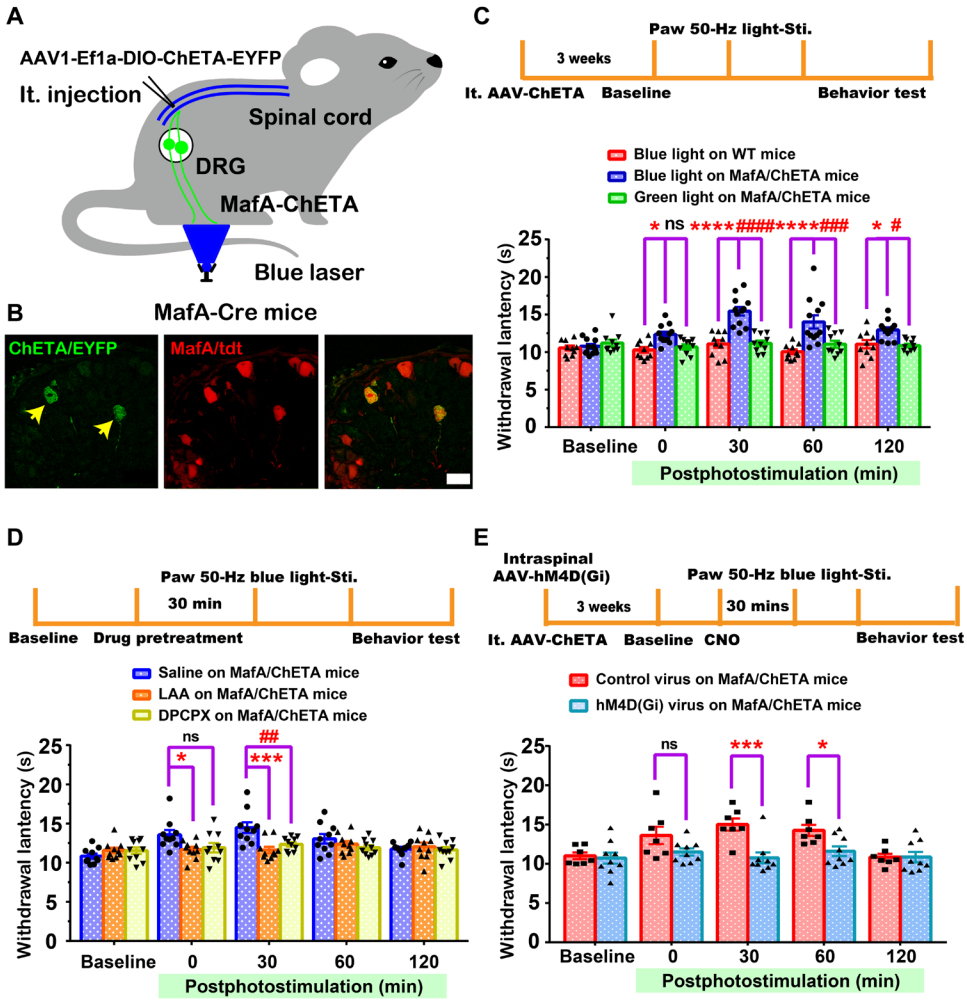

Fig. 6. Activation of astrocytes by Aβ-stimulation contributes to gate control of pain. (**A**) ChETA expression was induced in DRG neurons of MafA-Cre mice by intrathecal (It) AAV1-Ef1a-DIO-ChETA-EYFP virus injection 3 weeks before behavior testing. During behavior testing, 50-Hz blue laser light was shone directly onto the underside of the hind paw. (**B**) Staining shows virus expression in MafA/Tdtomato DRG neurons. Arrows indicate virus-infected DRG neurons. Scale bar, 50 μm. (**C**) Application of 50-Hz blue light, but not green light ($N = 10$ mice), inhibited heat pain in MafA-ChETA mice ($N = 12$ mice) at 30 min, as compared with that in the wild-type group ($N = 10$ mice). WT, wild type. (**D**) Pretreatment with LAA ($N = 10$ mice) or DPCPX ($N = 10$ mice), but not saline ($N = 10$ mice), blocked blue light–induced pain inhibition at the 30-min time point. (**E**) Pretreatment of GFAP-hM4D(Gi) mice ($N = 9$ mice) with CNO blocked blue light–induced pain inhibition at 30 and 60 min compared with that in the control-virus group ($N = 7$ mice). Data are presented as means ± SEM. *$P < 0.05$, ***$P < 0.001$, ****$P < 0.0001$, #$P < 0.05$, ##$P < 0.01$, ###$P < 0.001$, and ####$P < 0.0001$ versus the respective control groups by two-way mixed model ANOVA followed by Bonferroni post hoc comparisons.

such as glutamate and ATP to engage astrocytes. Astrocytes activated by Aβ-stimulation may act as a previously unknown nonneuronal gate for inhibiting spinal nociceptive transmission under physiologic conditions, in part through endogenous adenosinergic mechanisms (Fig. 7).

Astrocyte activation in the spinal cord was known to facilitate pain transmission or exacerbate pain. For example, noxious C-fiber stimulation activates astrocytes and thereby leads to pain hypersensitivity through glial release of cytokines such as interleukin-1β and tumor necrosis factor–α (*32*, *50*). Optogenetic activation of spinal astrocytes expressing ChR2 under the GFAP promoter also elicits mechanical hypersensitivity in naïve rats (*51*). Although previous studies have shown that astrocytes can have an inhibitory effect on synaptic transmission by enhancing the inhibitory interneuron activities in the brain, it is unclear that astrocytes play an inhibitory role in spinal cord synaptic transmission in the context of pain gate control (*52*, *53*). Here, we showed that activation of astrocytes by low-intensity Aβ-stimulation did not elicit pain but rather suppressed nociception in naïve mice. In this case, a subset of astrocytes in deeper laminae was activated first, followed by activation of superficial astrocytes. This activation profile differs from that induced by previous methods, which have activated a large population of astrocytes nonselectively (*51*). Thus, different astrocyte activation patterns may lead to differences in glial neurotransmitter and neuromodulator release, resulting in a reduction rather than facilitation of pain transmission. Another possibility is regional diversity of astrocytes in the CNS (*54*). On the basis of gene expression profiles, distinct, regionally restricted subtypes of astrocytes have been identified in the brain and spinal cord, implying different phenotypes and functions (*24*). A recent study showed a population of astrocytes located in the

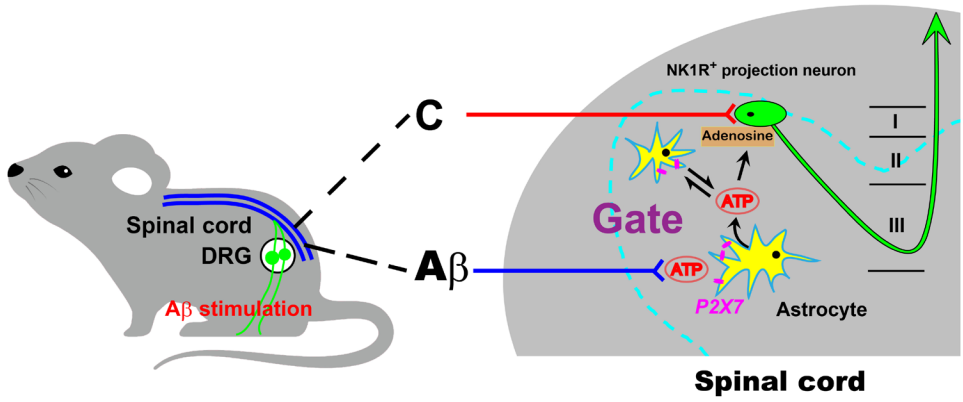

Fig. 7. Astrocyte-dependent gating mechanism of Aβ-stimulation. Astrocyte activation in the spinal cord of naïve mice by peripheral Aβ-stimulation generates synaptic LTD that leads to pain inhibition. This mechanism identifies a new role for spinal astrocytes in the physiologic gate control of pain. I, II, and III refer to laminae.

superficial spinal cord that is genetically defined by Hes5. One function of this astrocyte population is to gate descending noradrenergic control of mechanosensory behavior (*19*). It is possible that Aβ-stimulation in naïve animals activates a different subtype of astrocytes from that activated by noxious stimulation, thereby producing differing effects on pain.

A previously undescribed phenomenon that we observed was the propagation of astrocyte activation moving from deep laminae to the superficial layers after Aβ-stimulation. One possible underlying mechanism by which astrocyte activation might be propagated is release of diffusible glial transmitters such as ATP, which activates P2 nucleotide receptors expressed in neighboring astrocytes (*55*). Alternatively, chemical messengers might travel via nondiffusible mechanisms, such as gap junctions (*56*). Thus, this calcium wave from a subset of astrocytes in deeper laminae may spread and activate a wider range of astrocytes. Chemogenetic or optogenetic manipulations modulate astrocyte function independent of Ca^{2+} signaling via P2X7. We thus used these cell type–selective approaches to suppress astrocytes, as a complementary alternative to inhibiting P2X7 channels. Upon application of CNO, hM4Di activates the Gβγ subunit of the Gi protein, which then stimulates G protein inwardly rectifying potassium channels, causing an efflux of potassium. Photostimulation of halorhodopsin promotes an influx of chloride ions. These changes are expected to attenuate astrocyte activity directly and may also indirectly affect P2X7 activation. However, we cannot exclude the possibility that Aβ-fiber stimulation activates astrocytes indirectly by activating interneurons or other mechanisms. In future studies, different mouse genetic tools will be needed to investigate how Aβ-fiber stimulation activates interneurons.

ATP released by astrocytes can be readily converted into adenosine by ectonucleotidases in the extracellular space (*57*). Adenosine is an important neuromodulator that inhibits excitatory neurotransmission in the CNS, primarily by activating Gi-coupled presynaptic A1 receptors to reduce neurotransmitter release and by activating postsynaptic A1 receptors to decrease excitability (*58*, *59*). Thus, adenosine has the net effect of inhibiting spinal nociceptive transmission (*45*, *60*). Our findings indicate that nonneuronal pain gating governed by spinal astrocytes involves adenosinergic signaling. Nevertheless, other inhibitory mediators may also be at play. Activated astrocytes can release many glial neurotransmitters that modulate neuron excitability (*43*, *58*, *61*). For example, the inhibitory neurotransmitter GABA, which is very widely distributed in the CNS, can be released by both neurons and glial cells (*62*). Previous studies showed that astrocytes in the olfactory bulb (*63*), thalamus (*64*), and hippocampus (*52*, *53*, *65*) can inhibit neighboring neurons through the release of GABA. We found that activation of $GABA_A$ receptor, but not $GABA_B$ receptor, in the spinal cord also contributed to the inhibition of $NK1R^+$ neurons by Aβ-stimulation. Nevertheless, the roles of spinal GABAergic signaling in astrocyte-mediated pain gating remain to be investigated.

We are aware that both presynaptic mechanisms (e.g., reduced neurotransmitter release) and postsynaptic mechanisms (e.g., inhibition of dorsal horn neurons) may contribute to pain inhibitory effects from Aβ-stimulation. It is well known that glial cells are critical to maintaining homeostasis and modulating neuronal function in the CNS. It is possible that the nonneuronal pain inhibitory mechanism that we revealed may act in concert with these neuronal mechanisms. Future studies are needed to test whether astrocytes are involved in the neuronal mechanisms and whether these mechanisms are compromised if astrocytic activation by Aβ-stimulation is inhibited.

In summary, our findings indicate that a subset of spinal astrocytes is an important contributor to pain "gate" control under physiologic conditions. Astrocytes undergo morphologic and functional changes after injury, and astrogliosis in the spinal cord represents an important mechanism underlying chronic pain (*24*). Thus, it remains to be determined whether activation of astrocytes by Aβ-stimulation also leads to pain inhibition under pathologic pain conditions.

MATERIALS AND METHODS

Mouse lines

The NK1R-GFP-Cre mouse line was generated by using a homologous recombination knock-in approach. GFP-Cre transgene was integrated into the start codon of the NK1R gene using two homologous arms targeting the sequences of TTTGCTGCCTTGCCGCAAAATG and CTGAAAATTAAGAAAGTGCCC to replace the entire NK1R coding sequence. The MafA-Cre knock-in mouse line was generated by a CRISPR-Cas9 approach. The entire MafA

coding sequence was replaced with Cre transgene by using gRNAs targeting the 5′ region of the MafA gene CGCCGCCCGTCGGGG-CGCGGCCGGGCGCGGCGGCGGGGCTGGGGCCCCGG and the 3′ region of the Maf gene CCGGGGACAAGTTTGCGCAGG-CCGCCCCGGTCTCGGTTCAGACTCTGAGG. GFAP-Cre and ROSA26LSL-GCaMP6s mouse lines were acquired from the Jackson Laboratory (Bar Harbor, ME). We included both male and female mice in our study. All experiments were carried out with protocols approved by the Animal Care and Use Committee of the Johns Hopkins University School of Medicine.

Two-photon in vivo imaging

Mice were anesthetized with an intraperitoneal injection of pentobarbital (50 mg/kg), and spinal cord was exposed by dorsal laminectomy at the T12 level. We used 3% agarose to create a small well in which to place a 20× water immersion lens. Then, we carefully removed the dura mater and rotated the animal around the longitudinal axis by approximately 30° for imaging with the Scientifica Galvo Multiphoton System and Coherent Chameleon Ultra II laser. We tuned the laser at 900 nm for two-photon excitation for GCaMP6m and set the laser power to the lowest level (~20 mW) to avoid phototoxicity. Image resolution was 512 × 512 pixels. Calcium signal amplitudes are expressed as a ratio of fluorescence difference to basal fluorescence ($\Delta F/F$).

Spinal cord slice preparation

Four- to 6-week-old mice were deeply anesthetized with 2% isoflurane. Spinal cord with dorsal root was rapidly removed and placed in ice-cold, low-sodium Krebs solution, which contained 95 mM NaCl, 2.5 mM KCl, 26 mM $NaHCO_3$, 1.25 mM NaH_2PO_4-H_2O, 6 mM $MgCl_2$, 1.5 mM $CaCl_2$, 25 mM glucose, 50 mM sucrose, and 1 mM kynurenic acid, and was bubbled with 95% O_2/5% CO_2. We cut sagittal spinal cord slices (400 μm) with dorsal roots or DRG attached on a vibratome (VT1200, Leica Biosystems, Buffalo Grove, IL, USA) and transferred them to low-sodium Krebs solution without kynurenic acid for recovery at 34°C for 45 min and then at room temperature for an additional hour before we used them for experimental recordings.

Evoked EPSCs

Slices were stabilized with a nylon harp and submerged in a low-volume recording chamber (SD Instruments, San Diego, CA, USA), which was perfused with Krebs solution at a rate of 5 ml/min (125 mM NaCl, 2.5 mM KCl, 26 mM $NaHCO_3$, 1.25 mM NaH_2PO_4-H_2O, 1 mM $MgCl_2$, 2 mM $CaCl_2$, and 25 mM glucose) and bubbled with 95% O_2/5% CO_2. Thin-walled glass pipettes (World Precision Instruments, Sarasota, FL) fabricated with a puller (P1000; Sutter Instruments, Novato, CA) had resistances of 3 to 6 MΩ and were filled with an internal solution composed of 135 mM CsF, 5 mM CsCl, 5 mM EGTA, 10 mM Na-HEPES, 1 mM Mg-ATP, 0.1 mM Na–guanosine 5′-triphosphate, and 2 mM QX-314. Whole-cell patch-clamp recording of NK1-positive neurons was carried out under oblique illumination with an Olympus fixed-stage microscope system. Data were acquired with pClamp 10 software and a Multiclamp amplifier (Molecular Devices, Sunnyvale, CA). Membrane current signals were sampled at 10 kHz and low-pass filtered at 2 kHz. The P2X7 antagonist A438079 (10 μM), astrocyte-specific blocker LAA (1 mM), ATP-converting enzyme inhibitor ARL67156 (50 μM), adenosine A1 receptor blocker DPCPX (2 μM), microglia activity inhibitor minocycline (1 μM), $GABA_A$ receptor antagonist bicuculline (10 μM), and $GABA_B$ receptor antagonist CGP 52432 (10 μM) were applied to the bath solution 30 min before recording was begun. For hM4Di DREADD-dependent astrocyte silence recording, CNO (1 μM) was applied to the bath solution 30 min before recording was begun.

To evoke postsynaptic currents in $NK1R^+$ neurons, we delivered paired-pulse test stimulation to the dorsal root through a suction electrode, which consisted of two synaptic volleys (500 μA, 0.1 ms) 400 ms apart at a frequency of 0.05 Hz (3 tests/min), using a Master-9 Pulse Stimulator and Iso-Flex Stimulus Isolator. Paired-pulse test stimulation was used to calculate the paired-pulse ratio (second amplitude/first amplitude).

To differentiate monosynaptic and polysynaptic connections, we delivered 20 times C-fiber strength electrical stimulation at 1 Hz for C-fiber eEPSCs and 20 times Aβ-fiber strength electrical stimulation at 20 Hz for Aβ-fiber eEPSCs. Neurons with no failure in EPSCs were monosynaptically connected.

As in our previous study (*34*), the fastest component was considered to correspond to Aβ-fiber activation [conduction velocity (CV): 5.7 ± 1.2 m/s]. A slower component was referred to as the Aδ-compound action potential (CV: 1.6 ± 0.3 m/s). The slowest component was considered to correspond to C-fiber activation (CV: 0.7 ± 0.2 m/s). To evoke astrocyte activation, we delivered electrical Aβ-stimulation to the dorsal root through a suction electrode. Because Aβ-fibers project mainly into the deeper dorsal horn (e.g., laminae III to V), it is conceivable that Aβ-stimulation would activate astrocytes in the deeper laminae first. However, applying high-intensity electrical stimulation, which excites both A- and C-fibers in the dorsal root, activated astrocytes in both deep and superficial laminae nearly simultaneously. We also measured the distance (1.99 ± 0.13 mm) between the electrode stimulation site on the dorsal root and the superficial dorsal horn in the transverse spinal cord slice after recording.

Confocal spinal cord slice imaging

GFAP-GCaMP6 mice were deeply anesthetized with 2% isoflurane. Spinal cord with dorsal root was rapidly removed and cut into 400-μm slices, similar to the way that spinal cord slices were prepared for patch-clamp recording. The GFP signals from GCaMP6 mice were measured with a 700 Zeiss confocal microscope as an indicator of Ca^{2+} transients. For slice imaging, we measured the number of activated astrocytes in each 5 min and found a 122 ± 15–s delayed activation in superficial laminae after Aβ-stimulation.

Virus injection

Mice anesthetized by isoflurane underwent a laminectomy at the T13-L1 level. A fine glass capillary was inserted ~500 μm from the dorsal surface into the spinal cord, and 500 nl of AAV5-GFAP-hM4D(Gi)-mCherry virus or AAV5-GFAP104-mCherry was injected at 50 nl/min. Three weeks later, animals were used for patch-clamp recording.

The virus used for optogenetic Aβ-fiber activation was AAV1-Ef1a-DIO-ChETA-EYFP. This virus was injected intrathecally into mice (pretreated with 25% intravenous mannitol) 3 weeks before behavior tests.

Microdialysis

Mice anesthetized by isoflurane underwent a laminectomy at the T13-L1 level. The microdialysis probe (CMA Microdialysis AB,

Stockholm, Sweden) was inserted into the dorsal horn at a 30 degree angle. The probe was connected to a microperfusion pump and perfused with artificial cerebrospinal fluid at a flow rate of 1 μl/min. Samples were collected on ice after 2 hours of stabilization. ATP was detected by the ENLITEN ATP Assay System (FF2000, Promega, Madison, WI), and adenosine was detected by the Adenosine Assay Kit (KA4547, Abnova, Taipei City, Taiwan).

Behavior tests

For the Hargreaves test, mice were placed under a transparent plastic box (4.5 × 5 × 10 cm) on a 29°C transparent glass table. A light source placed under the transparent glass delivered a beam of light as a heat source to the hind paw. The latency for the animal to withdraw its hind paw was recorded. If no response occurred by 30 s, we terminated the test to prevent burns. All drugs were injected intrathecally 30 min before behavioral studies. Mechanical sensitivity was assessed with the von Frey test by the frequency method. Two calibrated von Frey monofilaments (0.4 and 1 g) were used. Each von Frey filament was applied perpendicularly to the plantar side of the hind paw for approximately 1 s; the stimulation was repeated 10 times to both hind paws. The occurrence of paw withdrawal in each of these 10 trials was expressed as a percent response frequency: paw withdrawal frequency = (number of paw withdrawals/10 trials) × 100%. All the behavioral observations were fully blinded.

For electrical stimulation, mice were anesthetized by isoflurane, and a stimulus electrode was inserted under the sciatic nerve. Aβ-stimulation of 50 Hz, 20 μA was applied for 10 min. A sham group was anesthetized and underwent electrode insertion, but no stimulation was applied. For optogenetic stimulation, a 50-Hz blue laser or green laser was applied to the hind paw through the transparent glass for 10 min. In any attempt to create a double knock-in mouse, the NK1R and MafA genes would interfere with each other because both are Cre transgenes. This technical limitation makes it nearly impossible to perform optogenetic activation in patch-clamp recordings or GCaMP imaging in our transgenic mice. Therefore, we performed $MafA^+$ optogenetic activation in pain behavior tests only as a proof of principle.

Immunofluorescence

Two- to 4-month-old mice were anesthetized with pentobarbital and perfused with 0.1 M phosphate-buffered saline followed by 4% formaldehyde. Spinal cord and DRG were collected and postfixed at 4°C for 2 hours. Tissues were cryoprotected in 30% sucrose overnight, sectioned with a cryostat, and placed on slides. The slides were incubated with primary antibodies overnight at 4°C and then with secondary antibody for 2 hours at room temperature. Primary antibodies included mouse anti-GFAP (MAB360, Millipore; 1:1000), goat anti–adenosine A1-R (C-19; sc-7500, Santa Cruz Biotechnology; 1:500), rabbit anti-CGRP (14959, Cell Signaling Technology; 1:1000), chicken anti-neurofilament (200 kDa; NF200; NFH7857983, Aves Labs; 1:1000), rabbit anti–substance P receptor antibody (NK1R, Ab5060, EMD Millipore; 1:500), rabbit anti-NeuN antibody (ab177487, Abcam; 1:1000), and rabbit IBA1 antibody (PA5-27436, Thermo Fisher Scientific; 1:500). Secondary antibodies included Alexa 488–conjugated goat anti-rabbit (A11008, Thermo Fisher Scientific; 1:500), Alexa 488–conjugated goat anti-mouse (A11001, Thermo Fisher Scientific; 1:500), Alexa 488–conjugated goat anti-chicken (A11039, Thermo Fisher Scientific; 1:500), and Alexa 488–conjugated donkey anti-goat (A11055, Thermo Fisher Scientific; 1:500). To detect IB4 binding, we incubated sections with Griffonia simplicifolia isolectin GS-IB4, Alexa Fluor 488 conjugate (I21411, Thermo Fisher Scientific; 1:500).

For the colocalization analysis, the Coloc 2 plugin from ImageJ was used to evaluate the degree of correlation between pairs of pixels in the red and green channels. The Pearson's CC (PCC), which measures the pixel-by-pixel covariance in the signal levels of two images, was used here. PCC values range from 1 for two images whose fluorescence intensities are perfectly, linearly related, to −1 for two images whose fluorescence intensities are perfectly, but inversely, related to one another. For each staining, we measured six regions of interest within the superficial spinal cord from six different slides.

Statistical analysis

Data are presented as means ± SEM. *N* represents the number of mice analyzed in behavior tests, two-photon imaging, confocal imaging, and microdialysis, and the number of slices or neurons in electrophysiology recording. The distribution of the variables in each experimental group was assumed to be normal. For most statistical comparisons of two groups, we used two-way analysis of variance (ANOVA) followed by Bonferroni post hoc comparisons according to the experimental design. A two-tailed, paired Student's *t* test was used for comparisons between pre- and post–Aβ-stimulation in microdialysis experiments. Extended power analysis was used to justify the sample size. On the basis of previous studies, we assumed an SD of 2 for behavior tests or 0.3 for electrophysiology recording and that a sample size of six animals or seven slices per group would provide 80% (or 90%) power to detect a difference of 4 s or 50% in outcome between two groups. No data were excluded. Differences were considered to be statistically significant at $P < 0.05$.

SUPPLEMENTARY MATERIALS

Supplementary material for this article is available at https://science.org/doi/10.1126/sciadv.abi6287

View/request a protocol for this paper from *Bio-protocol*.

REFERENCES AND NOTES

1. R. Melzack, P. D. Wall, Pain mechanisms: A new theory. *Science* **150**, 971–978 (1965).
2. T. Goroszeniuk, D. Pang, Peripheral neuromodulation: A review. *Curr. Pain Headache Rep.* **18**, 412 (2014).
3. W. D. Mauck, C. L. Hunt, O. O. Olatoye, N. S. Warner, T. J. Lamer, Spinal cord and peripheral nerve stimulation for painful disorders. *Adv. Anesth.* **37**, 163–186 (2019).
4. M. Schmelz, Neuronal sensitivity of the skin. *Eur. J. Dermatol.* **21** (Suppl. 2), 43–47 (2011).
5. M. F. Yam, Y. C. Loh, C. S. Tan, S. Khadijah Adam, N. Abdul Manan, R. Basir, General pathways of pain sensation and the major neurotransmitters involved in pain pegulation. *Int. J. Mol. Sci.* **19**, 2164 (2018).
6. A. J. Todd, Neuronal circuitry for pain processing in the dorsal horn. *Nat. Rev. Neurosci.* **11**, 823–836 (2010).
7. A. I. Basbaum, D. M. Bautista, G. Scherrer, D. Julius, Cellular and molecular mechanisms of pain. *Cell* **139**, 267–284 (2009).
8. A. J. Todd, M. M. McGill, S. A. Shehab, Neurokinin 1 receptor expression by neurons in laminae I, III and IV of the rat spinal dorsal horn that project to the brainstem. *Eur. J. Neurosci.* **12**, 689–700 (2000).
9. R. Wercberger, A. I. Basbaum, Spinal cord projection neurons: A superficial, and also deep, analysis. *Curr. Opin. Physiol.* **11**, 109–115 (2019).
10. P. W. Mantyh, S. D. Rogers, P. Honore, B. J. Allen, J. R. Ghilardi, J. Li, R. S. Daughters, D. A. Lappi, R. G. Wiley, D. A. Simone, Inhibition of hyperalgesia by ablation of lamina I spinal neurons expressing the substance P receptor. *Science* **278**, 275–279 (1997).
11. C. L. Weisshaar, B. A. Winkelstein, Ablating spinal NK1-bearing neurons eliminates the development of pain and reduces spinal neuronal hyperexcitability and inflammation from mechanical joint injury in the rat. *J. Pain* **15**, 378–386 (2014).

12. L. M. Mendell, Constructing and deconstructing the gate theory of pain. *Pain* **155**, 210–216 (2014).
13. R. D. Treede, Gain control mechanisms in the nociceptive system. *Pain* **157**, 1199–1204 (2016).
14. B. Duan, L. Cheng, S. Bourane, O. Britz, C. Padilla, L. Garcia-Campmany, M. Krashes, W. Knowlton, T. Velasquez, X. Ren, S. Ross, B. B. Lowell, Y. Wang, M. Goulding, Q. Ma, Identification of spinal circuits transmitting and gating mechanical pain. *Cell* **159**, 1417–1432 (2014).
15. H. Petitjean, S. A. Pawlowski, S. L. Fraine, B. Sharif, D. Hamad, T. Fatima, J. Berg, C. M. Brown, L. Y. Jan, A. Ribeiro-da-Silva, J. M. Braz, A. I. Basbaum, R. Sharif-Naeini, Dorsal Horn Parvalbumin Neurons Are Gate-Keepers of Touch-Evoked Pain after Nerve Injury. *Cell Rep.* **13**, 1246–1257 (2015).
16. S. Sun, Q. Xu, C. Guo, Y. Guan, Q. Liu, X. Dong, Leaky gate model: Intensity-dependent coding of pain and itch in the spinal cord. *Neuron* **93**, 840–853.e5 (2017).
17. B. Duan, L. Cheng, Q. Ma, Spinal circuits transmitting mechanical pain and itch. *Neurosci. Bull.* **34**, 186–193 (2018).
18. M. M. Halassa, P. G. Haydon, Integrated brain circuits: Astrocytic networks modulate neuronal activity and behavior. *Annu. Rev. Physiol.* **72**, 335–355 (2010).
19. Y. Kohro, T. Matsuda, K. Yoshihara, K. Kohno, K. Koga, R. Katsuragi, T. Oka, R. Tashima, S. Muneta, T. Yamane, S. Okada, K. Momokino, A. Furusho, K. Hamase, T. Oti, H. Sakamoto, K. Hayashida, R. Kobayashi, T. Horii, I. Hatada, H. Tozaki-Saitoh, K. Mikoshiba, V. Taylor, K. Inoue, M. Tsuda, Spinal astrocytes in superficial laminae gate brainstem descending control of mechanosensory hypersensitivity. *Nat. Neurosci.* **23**, 1376–1387 (2020).
20. D. A. Sahlender, I. Savtchouk, A. Volterra, What do we know about gliotransmitter release from astrocytes? *Philos. Trans. R. Soc. Lond. B Biol. Sci.* **369**, 20130592 (2014).
21. U. Lalo, O. Palygin, S. Rasooli-Nejad, J. Andrew, P. G. Haydon, Y. Pankratov, Exocytosis of ATP from astrocytes modulates phasic and tonic inhibition in the neocortex. *PLoS Biol.* **12**, e1001747 (2014).
22. N. B. Hamilton, D. Attwell, Do astrocytes really exocytose neurotransmitters? *Nat. Rev. Neurosci.* **11**, 227–238 (2010).
23. S. Lee, B. E. Yoon, K. Berglund, S. J. Oh, H. Park, H. S. Shin, G. J. Augustine, C. J. Lee, Channel-mediated tonic GABA release from glia. *Science* **330**, 790–796 (2010).
24. R. R. Ji, C. R. Donnelly, M. Nedergaard, Astrocytes in chronic pain and itch. *Nat. Rev. Neurosci.* **20**, 667–685 (2019).
25. R. R. Ji, A. Chamessian, Y. Q. Zhang, Pain regulation by non-neuronal cells and inflammation. *Science* **354**, 572–577 (2016).
26. E. D. Milligan, L. R. Watkins, Pathological and protective roles of glia in chronic pain. *Nat. Rev. Neurosci.* **10**, 23–36 (2009).
27. K. J. Sekiguchi, P. Shekhtmeyster, K. Merten, A. Arena, D. Cook, E. Hoffman, A. Ngo, A. Nimmerjahn, Imaging large-scale cellular activity in spinal cord of freely behaving mice. *Nat. Commun.* **7**, 11450 (2016).
28. K. Yoshihara, T. Matsuda, Y. Kohro, H. Tozaki-Saitoh, K. Inoue, M. Tsuda, Astrocytic Ca^{2+} responses in the spinal dorsal horn by noxious stimuli to the skin. *J. Pharmacol. Sci.* **137**, 101–104 (2018).
29. Y. Guan, P. W. Wacnik, F. Yang, A. F. Carteret, C. Y. Chung, R. A. Meyer, S. N. Raja, Spinal cord stimulation-induced analgesia: Electrical stimulation of dorsal column and dorsal roots attenuates dorsal horn neuronal excitability in neuropathic rats. *Anesthesiology* **113**, 1392–1405 (2010).
30. A. D. Hibell, E. J. Kidd, I. P. Chessell, P. P. Humphrey, A. D. Michel, Apparent species differences in the kinetic properties of P2X(7) receptors. *Br. J. Pharmacol.* **130**, 167–173 (2000).
31. H. Ikeda, J. Stark, H. Fischer, M. Wagner, R. Drdla, T. Jager, J. Sandkuhler, Synaptic amplifier of inflammatory pain in the spinal dorsal horn. *Science* **312**, 1659–1662 (2006).
32. M. T. Kronschlager, R. Drdla-Schutting, M. Gassner, S. D. Honsek, H. L. Teuchmann, J. Sandkuhler, Gliogenic LTP spreads widely in nociceptive pathways. *Science* **354**, 1144–1148 (2016).
33. F. Yang, Q. Xu, B. Shu, V. Tiwari, S. Q. He, L. P. Vera-Portocarrero, X. Dong, B. Linderoth, S. N. Raja, Y. Wang, Y. Guan, Activation of cannabinoid CB1 receptor contributes to suppression of spinal nociceptive transmission and inhibition of mechanical hypersensitivity by Aβ-fiber stimulation. *Pain* **157**, 2582–2593 (2016).
34. A. D. Sdrulla, Q. Xu, S. Q. He, V. Tiwari, F. Yang, C. Zhang, B. Shu, R. Shechter, S. N. Raja, Y. Wang, X. Dong, Y. Guan, Electrical stimulation of low-threshold afferent fibers induces a prolonged synaptic depression in lamina II dorsal horn neurons to high-threshold afferent inputs in mice. *Pain* **156**, 1008–1017 (2015).
35. H. Smits, M. van Kleef, J. Holsheimer, E. A. Joosten, Experimental spinal cord stimulation and neuropathic pain: Mechanism of action, technical aspects, and effectiveness. *Pain Pract.* **13**, 154–168 (2013).
36. Y. X. Chu, Y. Zhang, Y. Q. Zhang, Z. Q. Zhao, Involvement of microglial P2X7 receptors and downstream signaling pathways in long-term potentiation of spinal nociceptive responses. *Brain Behav. Immun.* **24**, 1176–1189 (2010).
37. C. Ficker, K. Rozmer, E. Kato, R. D. Ando, L. Schumann, U. Krugel, H. Franke, B. Sperlagh, T. Riedel, P. Illes, Astrocyte-neuron interaction in the substantia gelatinosa of the spinal cord dorsal horn via P2X7 receptor-mediated release of glutamate and reactive oxygen species. *Glia* **62**, 1671–1686 (2014).
38. M. Khurgel, A. C. Koo, G. O. Ivy, Selective ablation of astrocytes by intracerebral injections of alpha-aminoadipate. *Glia* **16**, 351–358 (1996).
39. B. Liu, M. Su, S. Tang, X. Zhou, H. Zhan, F. Yang, W. Li, T. Li, J. Xie, Spinal astrocytic activation contributes to mechanical allodynia in a rat model of cyclophosphamide-induced cystitis. *Mol. Pain* **12**, 174480691667447 (2016).
40. L. Yang, Y. Qi, Y. Yang, Astrocytes control food intake by inhibiting AGRP neuron activity via adenosine A1 receptors. *Cell Rep.* **11**, 798–807 (2015).
41. A. Kol, A. Adamsky, M. Groysman, T. Kreisel, M. London, I. Goshen, Astrocytes contribute to remote memory formation by modulating hippocampal-cortical communication during learning. *Nat. Neurosci.* **23**, 1229–1239 (2020).
42. Y. Guan, Q. Liu, Z. Tang, S. N. Raja, D. J. Anderson, X. Dong, Mas-related G-protein-coupled receptors inhibit pathological pain in mice. *Proc. Natl. Acad. Sci. U.S.A.* **107**, 15933–15938 (2010).
43. Y. Xiong, S. Sun, S. Teng, M. Jin, Z. Zhou, Ca^{2+}-Dependent and Ca^{2+}-Independent ATP Release in Astrocytes. *Front. Mol. Neurosci.* **11**, 224 (2018).
44. R. D. Fields, G. Burnstock, Purinergic signalling in neuron-glia interactions. *Nat. Rev. Neurosci.* **7**, 423–436 (2006).
45. M. W. Salter, J. L. Henry, Evidence that adenosine mediates the depression of spinal dorsal horn neurons induced by peripheral vibration in the cat. *Neuroscience* **22**, 631–650 (1987).
46. S. A. Levesque, E. G. Lavoie, J. Lecka, F. Bigonnesse, J. Sevigny, Specificity of the ecto-ATPase inhibitor ARL 67156 on human and mouse ectonucleotidases. *Br. J. Pharmacol.* **152**, 141–150 (2007).
47. M. J. Lohse, K. N. Klotz, J. Lindenborn-Fotinos, M. Reddington, U. Schwabe, R. A. Olsson, 8-Cyclopentyl-1,3-dipropylxanthine (DPCPX)--A selective high affinity antagonist radioligand for A1 adenosine receptors. *Naunyn Schmiedebergs Arch. Pharmacol.* **336**, 204–210 (1987).
48. A. Arcourt, L. Gorham, R. Dhandapani, V. Prato, F. J. Taberner, H. Wende, V. Gangadharan, C. Birchmeier, P. A. Heppenstall, S. G. Lechner, Touch receptor-derived sensory information alleviates acute pain signaling and fine-tunes nociceptive reflex coordination. *Neuron* **93**, 179–193 (2017).
49. L. A. Gunaydin, O. Yizhar, A. Berndt, V. S. Sohal, K. Deisseroth, P. Hegemann, Ultrafast optogenetic control. *Nat. Neurosci.* **13**, 387–392 (2010).
50. D. Gruber-Schoffnegger, R. Drdla-Schutting, C. Honigsperger, G. Wunderbaldinger, M. Gassner, J. Sandkuhler, Induction of thermal hyperalgesia and synaptic long-term potentiation in the spinal cord lamina I by TNF-α and IL-1β is mediated by glial cells. *J. Neurosci.* **33**, 6540–6551 (2013).
51. Y. Nam, J. H. Kim, J. H. Kim, M. K. Jha, J. Y. Jung, M. G. Lee, I. S. Choi, I. S. Jang, D. G. Lim, S. H. Hwang, H. J. Cho, K. Suk, Reversible liduction of pain hypersensitivity following optogenetic stimulation of spinal astrocytes. *Cell Rep.* **17**, 3049–3061 (2016).
52. M. Matos, A. Bosson, I. Riebe, C. Reynell, J. Vallee, I. Laplante, A. Panatier, R. Robitaille, J. C. Lacaille, Astrocytes detect and upregulate transmission at inhibitory synapses of somatostatin interneurons onto pyramidal cells. *Nat. Commun.* **9**, 4254 (2018).
53. J. Kang, L. Jiang, S. A. Goldman, M. Nedergaard, Astrocyte-mediated potentiation of inhibitory synaptic transmission. *Nat. Neurosci.* **1**, 683–692 (1998).
54. H. H. Tsai, H. Li, L. C. Fuentealba, A. V. Molofsky, R. Taveira-Marques, H. Zhuang, A. Tenney, A. T. Murnen, S. P. Fancy, F. Merkle, N. Kessaris, A. Alvarez-Buylla, W. D. Richardson, D. H. Rowitch, Regional astrocyte allocation regulates CNS synaptogenesis and repair. *Science* **337**, 358–362 (2012).
55. P. B. Guthrie, J. Knappenberger, M. Segal, M. V. Bennett, A. C. Charles, S. B. Kater, ATP released from astrocytes mediates glial calcium waves. *J. Neurosci.* **19**, 520–528 (1999).
56. S. Finkbeiner, Calcium waves in astrocytes-filling in the gaps. *Neuron* **8**, 1101–1108 (1992).
57. M. J. Zylka, Pain-relieving prospects for adenosine receptors and ectonucleotidases. *Trends Mol. Med.* **17**, 188–196 (2011).
58. J. M. Zhang, H. K. Wang, C. Q. Ye, W. Ge, Y. Chen, Z. L. Jiang, C. P. Wu, M. M. Poo, S. Duan, ATP released by astrocytes mediates glutamatergic activity-dependent heterosynaptic suppression. *Neuron* **40**, 971–982 (2003).
59. R. W. Greene, H. L. Haas, The electrophysiology of adenosine in the mammalian central nervous system. *Prog. Neurobiol.* **36**, 329–341 (1991).
60. T. H. Tam, M. W. Salter, Purinergic signalling in spinal pain processing. *Purinergic Signal.* **17**, 49–54 (2021).
61. R. D. Fields, Nonsynaptic and nonvesicular ATP release from neurons and relevance to neuron-glia signaling. *Semin. Cell Dev. Biol.* **22**, 214–219 (2011).
62. B. E. Yoon, C. J. Lee, GABA as a rising gliotransmitter. *Front. Neural Circuits* **8**, 141 (2014).
63. A. S. Kozlov, M. C. Angulo, E. Audinat, S. Charpak, Target cell-specific modulation of neuronal activity by astrocytes. *Proc. Natl. Acad. Sci. U.S.A.* **103**, 10058–10063 (2006).
64. C. Jimenez-Gonzalez, T. Pirttimaki, D. W. Cope, H. R. Parri, Non-neuronal, slow GABA signalling in the ventrobasal thalamus targets δ-subunit-containing GABAA receptors. *Eur. J. Neurosci.* **33**, 1471–1482 (2011).

65. K. Le Meur, J. Mendizabal-Zubiaga, P. Grandes, E. Audinat, GABA release by hippocampal astrocytes. *Front. Comput. Neurosci.* **6**, 59 (2012).

Acknowledgment: We thank D. Green, E. Sypek, and C. F. Levine at Johns Hopkins University for reading and editing the manuscript. We thank C. Wang, N. Bolduc, and D. Chang for assistance with generation and characterization of MafA-Cre CRISPR mice. **Funding:** This study was conducted at the Johns Hopkins University and was supported by the National Institutes of Health (Bethesda, Maryland, USA) grants NS054791 (X.D.), NS113883 (X.D.), NS110598 (Y.G.), NS117761 (Y.G.), DE022750 (M.J.C.), and DE022750-04S1 (L.K.C., M.C.); by the Lerner Family Fund for Pain Research (Q.H., Z.C., and M.J.C.); and by the Neurosurgery Pain Research Institute at Johns Hopkins University School of Medicine (Y.G. and M.J.C.). This work was facilitated by the Pain Research Core, which is funded by the Blaustein Fund and the Neurosurgery Pain Research Institute at the Johns Hopkins School of Medicine. **Author contributions:** Q.X. designed and performed most of the experiments and analyzed the data with assistance from N.C.F. and S.H. for microinjection, retrograde labeling, and immunostaining, M.A. for in vivo imaging, Q.H. for microdialysis, and Z.C. and F.Y. for in vivo electrophysiological recordings of dorsal horn neurons. M.J.C. and L.K.C. contributed to design and generation of MafA-Cre CRISPR mice. Q.X., Y.G., and X.D. wrote the manuscript with input from all authors. Y.G. and X.D. conceived and supervised the project. **Competing interests:** All authors declare that they have no competing interests. **Data and materials availability:** All data needed to evaluate the conclusions in the paper are present in the paper and/or the Supplementary Materials.

Submitted 23 March 2021
Accepted 14 September 2021
Published 3 November 2021
10.1126/sciadv.abi6287